On the Estimation of Doubly-Selective Fading Channels

Fengzhong Qu, *Student Member, IEEE*, and Liuqing Yang, *Senior Member, IEEE*

***Abstract*—Coherent communications over doubly-selective fading channels are attracting increasing research interests because of the performance advantage over their noncoherent counterparts. In this paper, we use a simple windowing and de-windowing technique to improve the accuracy of an existing basis expansion model (BEM) and develop a windowed least-squares (WLS) estimator for doubly-selective fading channels. We also design the optimum pilot pattern for the WLS estimator. Our designs can considerably improve the channel estimation performance. Simulations are provided to corroborate our theoretical analysis.**

***Index Terms*—Basis expansion model, discrete Fourier transform, window, least squares, channel estimation.**

I. Introduction

DOUBLY-SELECTIVE fading channels are more frequently encountered in wireless communications as the desired data rate and mobility grow simultaneously. They are also inherent in underwater acoustic channels with large fractional bandwidth and unstable propagation media. As a result, estimation of doubly-selective fading channels has been extensively studied in recent years (see e.g., [2], [3], [4], [1]).

In order to estimate the doubly-selective fading channels by using limited number of pilots, one immediate idea is to reduce the number of the coefficients to be estimated since the channel coefficients in time domain are typically highly correlated. Based on this idea, different basis expansion models (BEMs) have been proposed in previous work. The polynomial BEM in [1] approaches the real channel when the polynomial order approaches infinity. The Karhunen-Loève decomposition BEM in [4] requires channel statistics. The basis of the Slepian sequence BEM in [5] varies with the maximum Doppler. Though the discrete Fourier transform (DFT) BEM in [3] avoids these disadvantages, it suffers from high frequency leakage as we will analyze in detail later.

In this paper, we propose a simple windowing and de-windowing technique at the receiver to improve the precision of the DFT BEM, based on which we develop a windowed least-squares (WLS) channel estimator. In addition, we will show that the windowing and de-windowing technique will also improve the minimum mean square error (MMSE) estimators in [3]. In the literature, windowing techniques have been proposed in [2], [6] for channel estimation. However, in [2] the windowing operation is performed at the transmitter, which could affect the signal-to-noise ratio (SNR) of the symbols at the edges of the window with relatively small coefficients and in turn the bit error rate (BER) performance. Although [6] uses a window at the receiver, no detailed analysis or optimum pilot pattern design is given. In our approach, the windowing and de-windowing procedure is performed only at the receiver and only on the channel estimation branch. We also design the optimum pilot pattern. Analysis and simulations will be provided to verify the performance improvements of our simple estimator, in comparison with existing ones.

Notation: We will use boldface lowercase and uppercase letters for vectors and matrices, $[\boldsymbol{x}]_n$ and $[\boldsymbol{X}]_{n,m}$ for the nth element of vector $\boldsymbol{x}$ and the (n,m)th element of the matrix $\boldsymbol{X}$. $\mathbb{E}\{\cdot\}$ will be used for expectation, $\mathrm{tr}\{\boldsymbol{X}\}$ for the trace of matrix $\boldsymbol{X}$, $*$ for convolution, $\otimes$ for Kronecker product, superscript $\{\cdot\}^H$ for matrix Hermitian and $\{\cdot\}^T$ for matrix transposition. $\boldsymbol{I}_N$ denotes the $(N \times N)$ identity matrix, $\boldsymbol{0}_N$ denotes the $(N \times 1)$ zero vector, and $\mathcal{CN}(\mu, \sigma^2)$ denotes the complex Gaussian distribution with mean μ and variance σ^2.

II. System Model

Let $h(n;l)$ denote the discrete time-varying impulse response of the doubly-selective channel and $x(n)$ the transmitted signal. The received signal can be obtained by the linear time varying convolution of $x(n)$ and $h(n;l)$ in the presence of additive white Gaussian noise (AWGN) $z(n)$:

$$y(n) = \sum_{l=0}^{L} h(n;l)x(n-l) + z(n), \tag{1}$$

where $x(n)$ and $y(n)$ denote the nth transmitted and received symbol, and $L := \lfloor \tau_{max}/T_s \rfloor$ means the channel has $(L+1)$ delay taps with T_s being the symbol duration and τ_{max} the maximum delay spread. We adopt the wide-sense stationary uncorrelated scattering (WSSUS) assumption so that the channel coefficients from different delay taps are independent.

Due to the maximum moving speed limit, there is a maximum Doppler frequency f_{max}. The discrete-time Fourier transform (DTFT) of $h(n;l)$ given by $H(f;l) = \sum_{n=-\infty}^{\infty} h(n;l)e^{-2\pi nf}$ satisfies $H(f;l) = 0$ for $|f| > f_{max}$. In practice, however, one only has the observation of the channel over a finite block. Let N be the block size, $\boldsymbol{h}(l) := [h(1;l), ..., h(N;l)]^T$ be the $N \times 1$ truncated channel for the lth delay tap and the $(N \times N)$ diagonal matrix $\boldsymbol{W}$ with $[\boldsymbol{W}]_{k,k} = w(k) \neq 0$ be the window multiplied to the channel truncation. If it is a rectangular window, we have

Manuscript received May 9, 2008; revised June 28, 2008; accepted January 25, 2009. The associate editor coordinating the review of this letter and approving it for publication was J. Olivier.

The authors are with department of Electrical and Computer Engineering, University of Florida, P.O. Box 116130, Gainesville, FL 32611, USA (e-mail: jimqufz@ufl.edu, lqyang@ece.ufl.edu).

This work is in part supported by the National Science Foundation under grant No. ECS-0621879, and by the Office of Naval Research under grant No. N00014-07-1-0193. Part of the results in this paper was presented at CISS 2008, Princeton, NJ.

Digital Object Identifier 10.1109/TWC.2010.04.080631

$\boldsymbol{W} = \boldsymbol{I}_N$. Then, the time- and Doppler-domain relationship of the channel can be obtained as:

$$\boldsymbol{W}\boldsymbol{h}(l) = \boldsymbol{F}^H \tilde{\boldsymbol{g}}(l) = \boldsymbol{F}_P^H \tilde{\boldsymbol{g}}_P(l) + \boldsymbol{F}_{N-P}^H \tilde{\boldsymbol{g}}_{N-P}(l), \quad (2)$$

where $\boldsymbol{F}_P$ and $\boldsymbol{F}_{N-P}$ denote the P low-frequency and the $(N-P)$ high-frequency rows of the N-point DFT matrix $\boldsymbol{F}$; $\tilde{\boldsymbol{g}}(l) := [\tilde{g}(1;l), ..., \tilde{g}(N;l)]^T$ denotes the DFT of the windowed channel vector $\boldsymbol{W}\boldsymbol{h}(l)$; $\tilde{\boldsymbol{g}}_P(l)$ and $\tilde{\boldsymbol{g}}_{N-P}(l)$ denote the P low-frequency and the $(N-P)$ high-frequency components of $\tilde{\boldsymbol{g}}(l)$. With a rectangular window $\boldsymbol{W} = \boldsymbol{I}_N$, $P = 2\lceil f_{max} N T_s \rceil + 1$, which is simply calculated by f_{max} divided by the Doppler-domain resolution $(NT_s)^{-1}$ (sampling in Doppler domain) and $\tilde{\boldsymbol{g}}_{N-P}(l) = 0$, Eq. (2) becomes the DFT BEM used in [2], [3], where the high frequency components are simply set to zero. However, we will show next that this model is not accurate.

Let us treat the channel as random with each realization satisfying $H(f;l) = 0$ when $|f| > f_{max}$. It follows that the autocorrelation function of $H(f;l)$ in Doppler domain (f) satisfies $R_l(f,\phi) = 0$ when $|f| > f_{max}$. Actually, one of the classical methods to generate time-varying fading channels is to pass a white Gaussian random signal through a filter with a frequency response equal to the square-root of the desired Doppler spectrum required [7, Chapter 5]. Hence, we also assume that $R_l(f,\phi) = 0$ when $\phi \neq 0$.

Let $W(f)$ be the spectrum of the window function, we obtain the power spectrum density (PSD) of the windowed channel as:

$$\tilde{R}_l(f,0) = \mathbb{E}[\{H(f;l) * W(f)\}^2] = R_l(f,0) * |W(f)|^2. \quad (3)$$

Then, sampling in the Doppler domain at the interval of $(NT_s)^{-1}$, the PSD of the windowed channel becomes $\tilde{R}_l\left(\frac{k}{NT_s}, 0\right), k = 1, 2, ..., N$. This corresponds to the energy distribution of the channel in Doppler domain.

Notice that, however, $W(f)$ in Eq. (3) is never strictly band-limited. More specifically, if one simply truncates the signal or, equivalently, uses a rectangular window as in [3], $W(f)$ is a folded $sinc$ function. As a result, the PSD $\tilde{R}_l(f,0) \neq 0$ when $|f| > f_{max}$, which indicates that the truncating operation introduces high-frequency components in Doppler domain.

In fact, the average signal-to-interference ratio (SIR) can be defined as:

$$\text{SIR} := \frac{\sum_{k \notin (P/2, N-P/2)} \sum_{l=0}^{L} \tilde{R}_l\left(\frac{k}{NT_s}, 0\right)}{\sum_{k \in (P/2, N-P/2)} \sum_{l=0}^{L} \tilde{R}_l\left(\frac{k}{NT_s}, 0\right)}. \quad (4)$$

Eq. (4) implies that the SIR can be improved by better concentrating the channel energy on the low-frequency components. Clearly, the direct truncation in [3] is equivalent to a rectangular window, whose side lobes decay very slowly, leading to significant energy leakage into the high-frequency range. To design the optimum window that maximizes the SIR in Eq. (4), channel statistics $R_l(f,0)$ is required. Here, we consider the situation where the channel statistics are not available, since the BEM becomes unnecessary otherwise, as we will show in the next section. In this case, windows with lower side lobes are clearly desirable according to Eq. (4). Of course, windows with lower side lobes usually lead to a broader main lobe. This implies that P should be slightly larger than $(2\lceil f_{max} N T_s \rceil + 1)$. In the next section, we will introduce an improved LS estimator based on the windowing advantage discussed above.

III. WLS Estimator

A. MMSE or LS?

When the channel statistics are available, one can easily use the linear MMSE estimator introduced in [8, Chapter 12] with any number of pilot observations to interpolate $h(n;l)$, neither time-Doppler analysis nor BEM required. However, estimation of the channel statistics is often difficult because the statistics may change over time [9]. In particular, for underwater acoustic channels, there is even no proper model to characterize the channel since the channel appears to be neither Rayleigh nor Rician distributed [10]. Motivated by these, we propose a WLS estimator that does not require any channel statistics.

B. WLS Estimator Design

Now, we are ready to design an estimator to LS fit the $P(L+1)$ low-frequency components in the Doppler domain, P for each tap. Let us consider an N-symbol transmitted block with B pilot subblocks inserted and let N_b denote the length of the bth pilot subblock. In order to eliminate the interference between the pilots and the data, L zeros are inserted after each data and pilot subblock. As a result, the last L transmitted symbols in each block are zeros. Together with the L zeros from the previous block, the transmitted vector can be written as $\boldsymbol{x} = [\boldsymbol{0}_L^T, x(1), ..., x(N-L), \boldsymbol{0}_L^T]^T$ and the received $N \times 1$ vector $\boldsymbol{y} = [y(1), ..., y(N)]^T$ as $\boldsymbol{y} = \boldsymbol{H}\boldsymbol{x} + \boldsymbol{z}$, where $\boldsymbol{z}$ is the $N \times 1$ noise vector and $\boldsymbol{H}$ is the $N \times (N+L)$ channel matrix with $[\boldsymbol{H}]_{n,m} = h(n; n+L-m)$. With a window being multiplied to the received vector, the system I/O becomes:

$$\boldsymbol{W}\boldsymbol{y} = \boldsymbol{W}\boldsymbol{H}\boldsymbol{x} + \boldsymbol{W}\boldsymbol{z} = \tilde{\boldsymbol{H}}\boldsymbol{x} + \boldsymbol{W}\boldsymbol{z}, \quad (5)$$

where $\tilde{\boldsymbol{H}}$ is the $(N+L) \times N$ windowed channel matrix with entries $[\tilde{\boldsymbol{H}}]_{n,m} = w(n)h(n; n+L-m)$. With the time-Doppler relationship shown in Eq. (2), we have

$$\begin{aligned} \tilde{\boldsymbol{H}} &= \sum_{k=1}^{N} \boldsymbol{D}_k^H \tilde{\boldsymbol{G}}_k \\ &= \sum_{k \notin (P/2, N-P/2)} \boldsymbol{D}_k^H \tilde{\boldsymbol{G}}_k + \sum_{k \in (P/2, N-P/2)} \boldsymbol{D}_k^H \tilde{\boldsymbol{G}}_k, \end{aligned} \quad (6)$$

where $\boldsymbol{D}_k$ is the $N \times N$ diagonal matrix with the kth row of $\boldsymbol{F}$, and $\tilde{\boldsymbol{G}}_k$ is a Toeplitz matrix with the first column $[\tilde{g}(k;0), ..., \tilde{g}(k;L), 0, ..., 0]^T$. Here, the high-frequency and low-frequency components are separated. Stacking the windowed received symbols from the pilots, we obtain

$$\boldsymbol{W}_p \boldsymbol{y}_p = \sum_{k=1}^{N} \begin{bmatrix} \boldsymbol{D}_{k,1}^H \tilde{\boldsymbol{G}}_{k,1} \boldsymbol{u}_1 \\ \vdots \\ \boldsymbol{D}_{k,B}^H \tilde{\boldsymbol{G}}_{k,B} \boldsymbol{u}_B \end{bmatrix} + \boldsymbol{W}_p \boldsymbol{z}_p, \quad (7)$$

where $\boldsymbol{u}_b$ is the bth pilot subblock, $\boldsymbol{D}_{k,b}$ and $\tilde{\boldsymbol{G}}_{k,b}$ are the submatrices of $\boldsymbol{D}_k$ and $\tilde{\boldsymbol{G}}_k$ corresponding to $\boldsymbol{u}_b$. The subscript

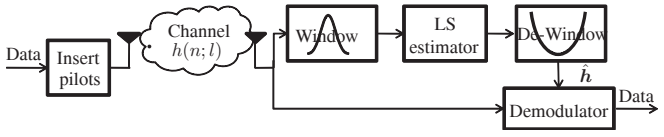

Fig. 1. Baseband equivalent system with the windowed least squares (WLS) estimator.

p denotes pilot. Since we need to LS fit the $P(L+1)$ low-frequency Doppler domain coefficients, the pilots need to be designed to make $\boldsymbol{y}_p$ a $P(L+1)\times 1$ vector. That is, $\sum_{b=1}^{B}(N_b+L)=P$. Due to the communtativity law of Toeplitz matrix and vector multiplication, we get $\tilde{\boldsymbol{G}}_{k,b}\boldsymbol{u}_b=\boldsymbol{U}_b\check{\boldsymbol{g}}(k)$, where $\boldsymbol{U}_b$ is an $(N_b+L)\times(L+1)$ Toeplitz matrix with the first column $\boldsymbol{u}_b$ padded by L zeros and $\check{\boldsymbol{g}}(k)=[\tilde{g}(k;0),...,\tilde{g}(k;L)]^T$. Eq. (7) can be rewritten as

$$\boldsymbol{W}_p\boldsymbol{y}_p=\sum_{k=1}^{N}\begin{bmatrix}\boldsymbol{D}_{k,1}^H\boldsymbol{U}_1\\ \vdots\\ \boldsymbol{D}_{k,B}^H\boldsymbol{U}_B\end{bmatrix}\check{\boldsymbol{g}}(k)=\boldsymbol{\Phi}\check{\boldsymbol{g}}+\boldsymbol{w}_p\boldsymbol{z}_p, \quad (8)$$

where $\check{\boldsymbol{g}}=[\check{\boldsymbol{g}}^T(1),...,\check{\boldsymbol{g}}^T(N)]^T$, and the $P(L+1)\times P(L+1)$ matrix $\boldsymbol{\Phi}$ is given by

$$\boldsymbol{\Phi}=\begin{bmatrix}\boldsymbol{D}_{1,1}^H\boldsymbol{U}_1 & \dots & \boldsymbol{D}_{N,1}^H\boldsymbol{U}_1\\ \vdots & \dots & \vdots\\ \boldsymbol{D}_{1,B}^H\boldsymbol{U}_B & \dots & \boldsymbol{D}_{N,B}^H\boldsymbol{U}_B\end{bmatrix}. \quad (9)$$

According to Eq. (6), we obtain:

$$\boldsymbol{W}_p\boldsymbol{y}_p=\boldsymbol{\Phi}_P\check{\boldsymbol{g}}_P+\boldsymbol{\Phi}_{N-P}\check{\boldsymbol{g}}_{N-P}+\boldsymbol{W}_p\boldsymbol{z}_p \quad (10)$$

where $\boldsymbol{\Phi}_P$ and $\check{\boldsymbol{g}}_P$ consist of $\boldsymbol{\Phi}(k)$ and $\check{\boldsymbol{g}}(k)$, with $k\le P/2$ or $k\ge N-P/2$; $\boldsymbol{\Phi}_{N-P}$ and $\check{\boldsymbol{g}}_{N-P}$ consist of $\boldsymbol{\Phi}(k)$ and $\check{\boldsymbol{g}}(k)$, with $P/2<k<N-P/2$. Notice that $\boldsymbol{\Phi}_P$ is a $P(L+1)\times P(L+1)$ square matrix with full rank. Considering the suppressed high-frequency components as interference in Eq. (10), we obtain the WLS estimate of $\check{\boldsymbol{g}}_P$ as:

$$\hat{\boldsymbol{g}}_P=\boldsymbol{\Phi}_P^{-1}\boldsymbol{W}_p\boldsymbol{y}_p. \quad (11)$$

Letting $\boldsymbol{h}=\left[\boldsymbol{h}^T(0),\boldsymbol{h}^T(1),...,\boldsymbol{h}^T(L)\right]^T$, $\tilde{\boldsymbol{g}}=\left[\tilde{\boldsymbol{g}}^T(0),\tilde{\boldsymbol{g}}^T(1),...,\tilde{\boldsymbol{g}}^T(L)\right]^T$ and $\boldsymbol{\Omega}=\boldsymbol{I}_{(L+1)}\otimes\boldsymbol{W}$, we obtain the time- and Doppler-domain relationship as:

$$\boldsymbol{h}=\boldsymbol{\Omega}^{-1}(\boldsymbol{I}_N\otimes\boldsymbol{F})^H\tilde{\boldsymbol{g}}=\boldsymbol{\Omega}^{-1}(\boldsymbol{I}_N\otimes\boldsymbol{F})^H\boldsymbol{\Theta}^T\check{\boldsymbol{g}}, \quad (12)$$

where the $N(L+1)\times N(L+1)$ interleaving matrix is given by $\boldsymbol{\Theta}:=\left[(\boldsymbol{I}_{(L+1)}\otimes\boldsymbol{e}_1)^T,\dots,(\boldsymbol{I}_{(L+1)}\otimes\boldsymbol{e}_N)^T\right]^T$ with $\boldsymbol{e}_k$ denoting the kth row of $\boldsymbol{I}_N$. For notational simplicity, defining $N(L+1)\times N(L+1)$ matrix $\boldsymbol{\Gamma}:=\boldsymbol{\Theta}(\boldsymbol{I}_N\otimes\boldsymbol{F})$, we can rewrite Eq. (12) as:

$$\begin{aligned}\boldsymbol{h}&=\boldsymbol{\Omega}^{-1}\boldsymbol{\Gamma}^H\check{\boldsymbol{g}}\\ &=\boldsymbol{\Omega}^{-1}\boldsymbol{\Gamma}_P^H\check{\boldsymbol{g}}_P+\boldsymbol{W}^{-1}\boldsymbol{\Gamma}_{N-P}^H\check{\boldsymbol{g}}_{N-P}\\ &\approx\boldsymbol{\Omega}^{-1}\boldsymbol{\Gamma}_P^H\check{\boldsymbol{g}}_P,\end{aligned} \quad (13)$$

where $\boldsymbol{\Gamma}_P=\boldsymbol{\Theta}_P\boldsymbol{I}_{(L+1)}\otimes\boldsymbol{F}_P$ and $\boldsymbol{\Gamma}_{N-P}=\boldsymbol{\Theta}_{N-P}\boldsymbol{I}_{(L+1)}\otimes\boldsymbol{F}_{N-P}$. $\boldsymbol{\Theta}_P$ is re-constructed from $\boldsymbol{\Theta}$ by taking columns $\boldsymbol{e}_k$, $k\le P/2$ or $k\ge N-P/2$, and $\boldsymbol{\Theta}_{N-P}$ by taking $\boldsymbol{e}_k^T$, $P/2<k<N-P/2$. It is easy to check $\boldsymbol{\Gamma}\boldsymbol{\Gamma}^H=\boldsymbol{\Gamma}^H\boldsymbol{\Gamma}=\boldsymbol{I}_{N(L+1)}$ and $\boldsymbol{\Gamma}_P\boldsymbol{\Gamma}_P^H=\boldsymbol{I}_{P(L+1)}$. At the last step of Eq. (13), the high-frequency components in the Doppler domain are considered as negligible interference. Thus, from Eq. (11) and (13), we obtain the channel estimate as

$$\hat{\boldsymbol{h}}=\boldsymbol{\Omega}^{-1}\boldsymbol{\Gamma}_P^H\boldsymbol{\Phi}_P^{-1}\boldsymbol{W}_p\boldsymbol{y}_p. \quad (14)$$

In Eq. (14), we can see that our WLS estimator performs the windowing and de-windowing procedure only at the receiver, and only on the pilots, affecting neither the data transmission pattern nor the demodulator. The system with our WLS channel estimator is illustrated in Fig. 1.

With this WLS estimator ready, a natural question will arise: what is the optimum pilot pattern?

C. Optimum Pilot Pattern Design

The optimum pilot pattern is designed to minimize the MSE of channel estimation. The MSE is given by:

$$\mathrm{MSE}=\mathbb{E}\{\|\boldsymbol{h}-\hat{\boldsymbol{h}}\|^2\}=\mathrm{MSE}_{N-P}+\mathrm{MSE}_z, \quad (15)$$

where

$$\mathrm{MSE}_{N-P}=\mathbb{E}\left\{\left\|\boldsymbol{\Omega}^{-1}\left[\boldsymbol{\Gamma}_{N-P}^H-\boldsymbol{\Gamma}_P^H\boldsymbol{\Phi}_P^{-1}\boldsymbol{\Phi}_{N-P}\right]\check{\boldsymbol{g}}_{N-P}\right\|^2\right\} \quad (16)$$

denotes the MSE resulted from the high-frequency components in the Doppler domain and

$$\mathrm{MSE}_z=\mathbb{E}\left\{\left\|\boldsymbol{\Omega}^{-1}\boldsymbol{\Gamma}_P^H\boldsymbol{\Phi}_P^{-1}\boldsymbol{W}_p\boldsymbol{z}_p\right\|^2\right\} \quad (17)$$

denotes the MSE resulted from AWGN.

In Eq. (16), since the windows with lower side lobes are bell-shaped in time domain suppressing the signals at either edge of the truncated signal block, MSE_{N-P} is actually a weighted summation of individual square errors, with inverse bell-shaped weights in the time domain. Hence, the resultant weighted MSE at the center of the windowed truncation is smaller than the edges. This motivates us to only retain the results at the center, and to use a sliding window to cover the entire time domain. Therefore, all the pilot subblocks are of identical importance. The pilot subblocks should then be identical and so are the spaces between the pilot subblocks.

Next, let us determine how many pilots each pilot subblock should have and how they should be placed. As we are retaining the estimation results for the center symbols of each sliding block, where the window weight is approximately 1, with the total pilot energy $\mathcal{E}P$, we obtain:

$$\begin{aligned}\mathrm{MSE}_z&\approx\mathbb{E}\left\{\left\|\boldsymbol{\Gamma}_P^H\boldsymbol{\Phi}_P^{-1}\boldsymbol{z}_p\right\|^2\right\}\\ &=\mathrm{tr}\left\{\mathbb{E}\left[\boldsymbol{\Gamma}_P^H\boldsymbol{\Phi}_P^{-1}\boldsymbol{z}_p\boldsymbol{z}_p^H(\boldsymbol{\Phi}_P^{-1})^H\boldsymbol{\Gamma}_P\right]\right\}\\ &=\sigma_z^2\mathrm{tr}\left\{\boldsymbol{\Phi}_P^{-1}(\boldsymbol{\Phi}_P^{-1})^H\right\}\ge\sigma_z^2NP/\mathcal{E}.\end{aligned} \quad (18)$$

The last step is derived with a similar procedure in [11]. The equality at the last step holds if and only if $\boldsymbol{\Phi}_P^{-1}(\boldsymbol{\Phi}_P^{-1})^H$ is a diagonal matrix with identical diagonal entries. Therefore, the optimum pilot pattern is the one with only 1 nonzero pilot in each pilot subblock and a total P such pilots in a block, as illustrated in Fig. 2. It is worth noting that this design coincides with the one in [3].

TABLE I
SIMULATION PARAMETERS

$f_{max} = 10$Hz	$T_s = 1/6000$s	$\tau_{max} = 10$ms	$L = 60$
$N = 1800$	$P = 9$	$2\lceil f_{max} N T_s \rceil + 1 = 7$	$\mathbb{E}\left\{\sum_{l=0}^{L} \|h(n;l)\|^2\right\} = 1$
Pilot Energy= 61	Channel delay profile: $s(l) = e^{-0.1l}$	Modulation: QPSK	Demodulation Equalizer: MMSE

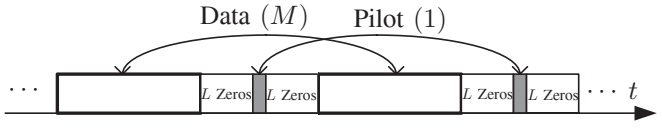

Fig. 2. The optimum training pattern.

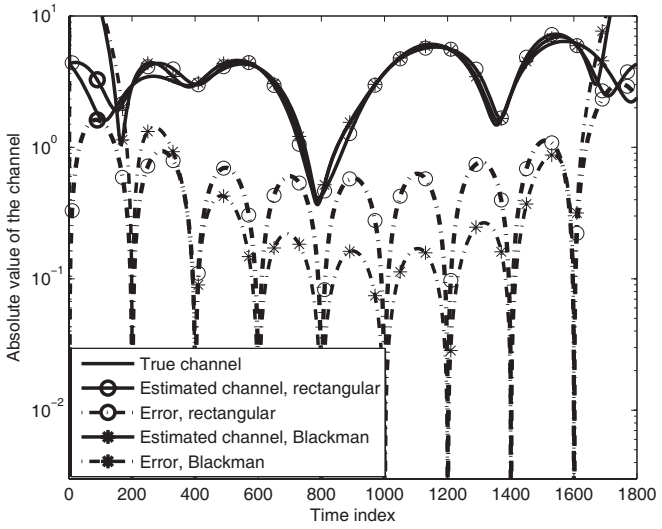

Fig. 3. One snapshot of the WLS estimation results.

D. Discussions

So far, we have established our WLS estimator with a simple windowing and de-windowing technique to improve the performance. In fact, our windowing and de-windowing technique, together with the DFT BEM, can be regarded as an improved BEM. We have proved that our improved BEM approximates the real channel more precisely than the original DFT BEM by suppressing the energy of high-frequency components that are regarded as interference. Hence, it is not surprising that the windowing technique helps improving the LS estimator. Actually, our windowed BEM is expected to help improve other BEM-based estimators, such as the MMSE estimator in [3], as we will confirm by simulations next.

IV. Simulation Results

In this section we use Jakes' model to test the performance of our WLS estimators. We simulate a typical underwater acoustic environment with carrier frequency $12k$Hz and transceiver moving velocity 1.3m/s or 2.4knots. The simulation parameters are summarized in Table I.

Fig. 3 shows one realization of our WLS estimator in the absence of AWGN. WLS estimators with a Blackman window and with a rectangular window are compared. Our WLS estimator fits the real channel much better in the center. In addition, we also observe that even with a rectangular window, the channel estimation error for the data time slots in the center is also smaller than the edges. The reason is that the channel estimates of the entire block are obtained from those of the pilots using a procedure reminiscent of interpolation, and that the center of the block benefits from the pilots on both sides.

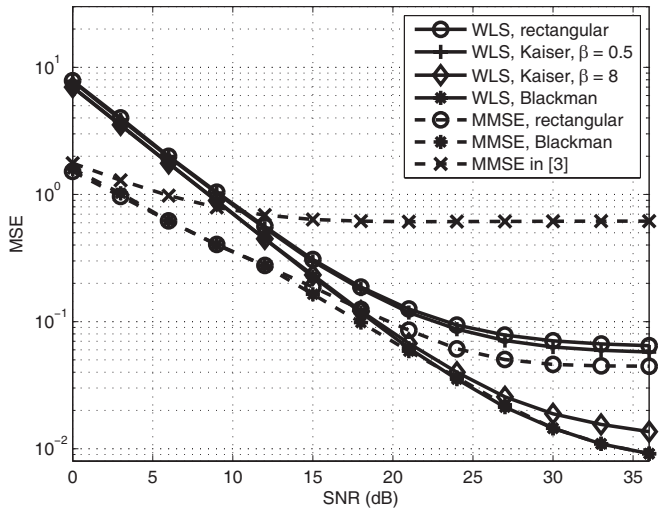

Fig. 4. MSE vs. SNR performance of the WLS and the MMSE channel estimators.

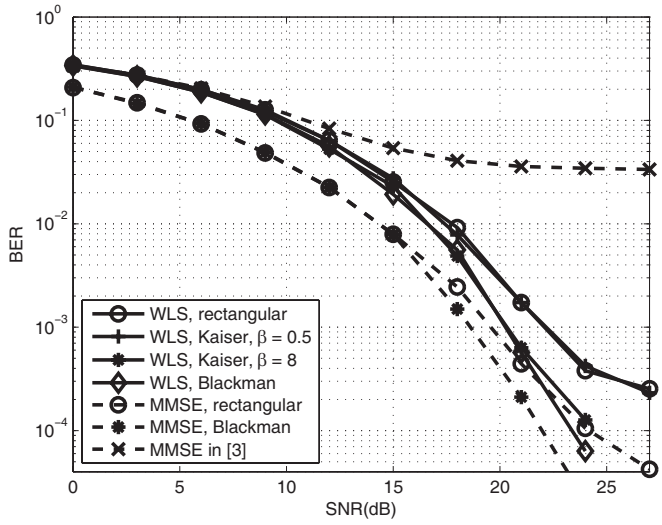

Fig. 5. BER vs. SNR performance of the WLS and the MMSE channel estimators.

Figs. 4 and 5 show the MSE and BER performance of several different estimators. We use a sliding window for our WLS scheme, and only take the estimation and demodulation results between the 2 center pilots. Notice that among the 4 different windows, Blackman window gives the best perfor-

mance, and rectangular the worst. This justifies our analysis in Section III. If the channel statistics are available, the MMSE estimator in [3] can be adopted. In addition to the fixed rectangular window (direct truncation) in [3], we also tested this MMSE estimator with our sliding window approach. From Figs. 4 and 5, we have the following observations:

i) In terms of channel estimation MSE, the MMSE estimators outperform the LS ones at low SNR, by taking advantage of the channel statistics. However, this MSE advantage does not seem to directly carry over to the BER comparisons. In Fig. 5, we observe that the BER performance of [3] is identical with the WLS estimators at low SNR, despite its MSE advantage shown in Fig. 4.
ii) The scheme in [3] results in the worst performance among all MMSE estimators. This confirms the advantage of our sliding window approach. Since the schemes with sliding window only take the results between the 2 center pilots, they require P times computation as the ones with fixed windows, but without altering the transceiver architecture.
iii) The MMSE estimators with rectangular windows are worse than appropriately windowed LS estimators at high SNR. In particular, the scheme in [3] with a fixed rectangular window is worse than all WLS estimators even at medium SNR. This confirms that our simple windowed approach not only helps LS estimators, but also MMSE ones.

V. Conclusions

In this paper, we proposed a WLS estimator for doubly-selective fading channels. We showed that the precision of the DFT BEM can be improved by a simple windowing and de-windowing procedure, which is applied only at the receiver and only to the pilots. We also designed the optimum pilot pattern. In addition, our simulations confirmed that the simple windowing and de-windowing procedure improves the performance of the existing BEM-based MMSE channel estimators as well.

References

[1] D. Borah and B. T. Hart, "Frequency-selective fading channel estimation with a polynomial time-varying channel model," *IEEE Trans. Commun.*, vol. 47, no. 6, pp. 862–873, June 1999.

[2] P. Jarvensivu, M. Matinmikko, and A. Mammela, "Signal design for LS and MMSE channel estimators," in *Proc. 13th IEEE International Symposium on Personal, Indoor and Mobile Radio Communications*, vol. 2, Lisboa, Portugal, Sep. 2002, pp. 956–960.

[3] X. Ma, G. B. Giannakis, and S. Ohno, "Optimal training for block transmissions over doubly selective wireless fading channels," *IEEE Trans. Signal Process.*, vol. 51, no. 5, pp. 1351–1366, May 2003.

[4] Q. T. Zhang, X. Y. Zhao, Y. X. Zeng, and S. H. Song, "Efficient estimation of fast OFDM channel," in *Proc. Intl. Conf. on Communications*, Istanbul, Turkey, Sep. 2006, pp. 4601–4605.

[5] T. Zeman and C. F. Mecklebräuker, "Time-variant channel estimation using discrete prolate spheroidal sequences," *IEEE Trans. Signal Process.*, vol. 53, no. 9, pp. 3597–3607, Sep. 2005.

[6] G. Leus, "On the estimation of rapidly time-varying channels," in *Proc. Euro. Signal Process. Conf. (EUSIPCO)*, Vienna, Austria, Sep. 2004, pp. 2227–2230.

[7] T. S. Rappaport, *Wireless Communications*. Prentice Hall, 2002.

[8] S. M. Kay, *Fundamentals of Statistical Signal Processing, Volume I: Estimation Theory*. Prentice-Hall, 1993.

[9] D. Schafhuber, G. Matz, and F. Hlawatsch, "Kalman tracking of time-varying channels in wireless MIMO-OFDM systems," in *Proc. 37th Asilomar Conf. Signals, Systems, Computers*, Pacific Grove, CA, Nov. 2003, pp. 1261–1265.

[10] W. B. Yang and T. C. Yang, "Characterization and modeling of underwater acoustic communications channels for frequency-shift-keying signals," in *Proc. MTS/IEEE Oceans Conf.*, Boston, MA, USA, Sep. 2006, pp. 1–6.

[11] T. L. Tung, K. Yang, and R. E. Hudson, "Channel estimation and adaptive power allocation for performance and capacity improvement of multiple-antenna OFDM systems," in *Proc. 3rd IEEE Signal Process. Workshop Signal Process. Adv. Wireless Commun.*, Taoyuan, Taiwan, Sep. 2001, pp. 82–85.